

Fermilab

TM-1137
1183.000
Sept. 1982

Proton Therapy Nozzles Design and Analysis

S. L. Kramer

Argonne National Laboratory

I. Introduction

Beams from high energy accelerators are constrained to have very small emittances. To be useful for large volume proton therapy they must be spread out in space to illuminate the entrance portal uniformly. This could be done by letting the beam diverge (either from its own angular spread or by defocusing it with quadrupoles) and then collimating the beam to a uniformity of the spatial density of particles to yield the required dose uniformity. However, this technique is very inefficient on the use of incident beam.

Although scanning the beam magnetically could yield high efficiency and highly uniform dose,¹ considerable development would be necessary to develop the technique and its required reliability. The use of multiple scattering foils simplifies the treatment planning and verification, since the size and uniformity is determined only by the properties of the materials and not by the variables (current, temperature, hysteresis, etc.) in magnetic scanning devices.

II. Multiple Scattering of High Energy Protons

Although an accurate description of the multiple scattering distribution is quite complex,² considerable simplification can be made by assuming a Gaussian distribution in r

$$f(r) \, r dr d\phi = \frac{1}{\pi R^2} \text{EXP} \left[-\left(\frac{r}{R}\right)^2 \right] r dr d\phi \quad (1)$$

where R = the root-mean-square radius of particle density measured a distance Z from the foil.

This distribution yields the probability that a proton in a pencil beam of particles will be scattered into an area $r dr d\phi$, transverse to the beam. The parameter R can be expressed in terms of an rms scatter angle $\langle \theta^2 \rangle^{1/2}$ by

$$R = Z \langle \theta^2 \rangle^{1/2} \quad (2)$$

For a differential thickness of material, dX , the mean square scatter angle is given approximately³ by

$$d\theta^2 = \left(\frac{E_s}{p\beta}\right)^2 \frac{dX}{X_R}$$

where p = the momentum of the proton
 β = the velocity factor
 X_R = the radiation length of the material and
 E_s = a constant of the material (≈ 17 to 21 MeV/c depending on Z ,
value used = 20 MeV/c)

For thick foils the mean square scatter angle is

$$\langle \theta^2 \rangle = \frac{E_s^2}{X_R} \int_0^X d\theta^2 = \frac{E_s^2}{X_R} \int_0^X \frac{dX}{(p\beta)^2} \quad (3a)$$

where the integration over X takes into account the change in $p\beta$. For thin foils ($p\beta \approx \text{constant}$)

$$\langle \theta^2 \rangle \approx \left(\frac{E_s}{p\beta} \right)^2 \frac{\Delta X}{X_R} \quad (3b)$$

For thick foils, Eq. (3a) can be solved⁴ by approximating the range energy relation by

$$E = KR^n$$

where K and n are constants
 E = the kinetic energy (MeV) and
 R = the mean range of the particles in gm/cm^2

Then the residual energy after passing through a thickness, X is given by

$$E_r = K(R - X)^n \quad (4)$$

For non-relativistic particles

$$p\beta \approx 2E_r = 2K(R - X)^n \quad (5)$$

With this approximation the mean square scatter angle is given substituting Eq. (5) into Eq. (3a) and integrating⁴

$$\langle \theta^2 \rangle = \frac{E_s^2}{4K^2 X_R (2n-1)} [(R-X)^{1-2n} - R^{1-2n}] \quad (6)$$

This expression is accurate to better than 10% below 200 MeV for protons.

For a fixed $\langle \theta^2 \rangle$ then the energy loss in the thickness ΔX is given approximately by

$$\Delta E \approx \frac{dE}{dX} \Big|_{E_0} \Delta X = -\frac{dE}{dX} \Big|_{E_0} \left(\frac{E_s}{p\beta} \right)^{-2} X_R \langle \theta^2 \rangle \quad (7)$$

and is proportional to the radiation length times the energy loss rate for the material. Table I lists reasonable values for n, K, X_R and the range of values for the relative energy loss ($\Delta E / \Delta E_{H_2O}$) for a fixed $\langle \theta^2 \rangle$, possible from different materials. Thus not only can the foil scatter the beam for dose uniformity but a coarse change of the distal edge Bragg peak can result from changes in the foil material.

Fig. 1 shows the multiple scattering distribution for a single scatter foil. In order that the dose distribution is uniform to $\pm 2.5\%$ the tumor area must have a radius such that

$$r \leq 0.23 R = 0.23 Z \langle \theta^2 \rangle^{1/2} \quad (8)$$

and collimators then eliminate the beam outside this area. The fraction of the beam inside this area is only 5% of the beam incident on the foil. For small tumor volumes this method can be used but the 95% of the beam lost in the collimators must have adequate shielding to reduce the radiation from secondary neutron exposure to the patient. Table II lists parameters for two field sizes (3 cm and 8 cm diameter) for a one meter nozzle length with a dose uniformity of $\pm 2.5\%$ inside the field volume (efficiency = 5%). The quantity ΔX_{H_2O} lists the reduction of the depth of penetration (in cm of H_2O) from the 25.5 cm penetration depth of the incident 200 MeV beam.

The obvious problem is that for field sizes greater than 3 cm diameter, the energy loss in the foil reduces the depth of penetration such that the beam is of little use. For fields larger than 3 cm diameter, the 3 cm field parameters can be used and the nozzle length scaled in proportion to the field diameter.

III. High Efficiency Nozzles

One way to improve the depth of penetration is to allow the protons to drift further, therefore requiring less energy loss in the scatter foil. However another method using two foils can help reduce the energy loss and

increase the efficiency. This method was suggested by Koehler⁵ and uses a beam stop to reduce the intensity in the center of the beam scattered from the first foil and a second foil to fill in the occluded areas.

Fig. 2 shows the arrangement of the foils and beam stops. If the beam distribution from the first foil is

$$f(r_1)r_1 dr_1 d\theta = \frac{1}{\pi R_1^2} \text{EXP} \left[- \left(\frac{r_1}{R_1} \right)^2 \right] r_1 dr_1 d\theta \quad (9)$$

where

$$R_1 = Z_1 \langle \theta_1^2 \rangle^{1/2}$$

then the second scatter foil yields a second and independent divergence $f(r_2)$ such that

$$\vec{r} = \vec{r}_1 + \vec{r}_2 \quad \text{or} \quad \vec{r}_2 = \vec{r} - \vec{r}_1$$

Now the conditional distribution

$$f(\vec{r}_1, \vec{r}_2) = f(\vec{r}_1) f(\vec{r}_2)$$

or

$$f(r_1, r) r dr d\theta r_1 dr_1 d\theta_1 = \frac{1}{(\pi R_1 R_2)^2} \text{EXP} \left\{ - \left(\frac{r_1}{R_1} \right)^2 - \left(\frac{r_1^2 + r^2}{R_2^2} \right) + \frac{2r_1 r}{R_2^2} \cos \theta \right\} r dr d\theta r_1 dr_1 d\theta_1$$

Integrating over \vec{r}_1 and θ yields the net beam distribution function in r

$$f(r) = \frac{2}{\pi R_1^2 R_2^2} \text{EXP} \left[-\left(\frac{r}{R_2}\right)^2 \right] \int_A \text{EXP} (-Kx^2) I_0 \left(\frac{2Xr}{R_2} \right) x dx \quad (10)$$

where

$$x = \frac{r_1}{R_2}, \quad K = 1 + \left(\frac{R_2}{R_1}\right)^2 .$$

$$I_0(Z) = \frac{1}{\pi} \int_0^\pi \text{EXP} (Z \cos \theta) d\theta$$

= Bessel Function I_0

The integration in Eq. (10) is over the disconnected region, A, where the beam is not stopped by the beam stops, i.e., the integration is for

$$0 \leq r_1 \leq A_0 \quad \text{and} \quad A_1 \leq r_1 \leq A_2$$

where A_0 , A_1 and A_2 are the projected radii of the beam stops on the entrance portal.

Equation (10) can be solved assuming values for R_1 , R_2 , A_0 , A_1 and A_2 . Since A_1 will set the approximate dimension of the uniform dose region, it is convenient to scale R_1 , R_2 , A_0 and A_2 by A_1 . The uniform dose region can then be defined in units of A_1 . When an optimum choice of these parameters is found A_1 can be scaled such that the uniform dose region corresponds to the tumor area to be covered. Finally the choice of Z_1 and Z_2 can be made to yield a reasonable depth of penetration by reducing the foil thickness. Fig. 3 and 4 show the dose distribution and beam efficiency distribution for two

choices of R_1 , R_2 , A_0 and A_2 . Fig. 3 uses a solid inner beam stop (i.e., $A_0 = a_0 = 0$) and yields a dose uniformity of $\pm 2.5\%$ for $r \leq 1.2 A_1$, and an efficiency of 14%. By opening a small hole in the inner beam stop (i.e., $A_0 \neq 0$) increased beam efficiency can be obtained. Fig. 4 demonstrates this type of nozzle, which has a dose uniformity of $\pm 2.5\%$ for $r \leq 1.45 A_1$ and an efficiency of 27%. Although other parameters might improve this efficiency slightly, this nozzle design is quite adequate. Table III lists the parameters for the nozzle shown in Fig. 4 for various field sizes of the $\pm 2.5\%$ dose uniformity region. The distances assumed for the nozzles described in Table III are $Z_1 = 5$ meters and $Z_2 = 4$ meters. The different materials used for the scattering foils offer a wide range of penetration depths. Additional variations in penetration depth is possible by changing material of only one of the two foils.

For the small field volumes a two scattering foil nozzle, as shown in Fig. 4, can be used but with a shorter nozzle length than shown in Table III. Table IV shows such nozzle parameters for small fields (≤ 20 cm diameter) with $Z_1 = 2$ meters and $Z_2 = 1$ meter. Although the smaller fields can be obtained by collimating the tumor area to be treated at the patient, the nozzles described in Table IV yield higher efficiency and reduced scatter dose from secondary neutrons off the collimators.

IV. Construction and Use of the High Efficiency Proton Nozzles

The actual use of these nozzles will be to choose a field size which yields adequate coverage of the tumor area, yet small enough to yield a reasonable dose rate. Then a beam stopping collimator (thickness = 2.5" Fe or

2" Pb) with hole radii given by Table III or IV (a_0 , a , and a_2) is inserted at the second scatter foil position. After the treatment plan has prescribed the distal edge of the tumor to be treated, the scatter foil material, given by Table III or IV, is chosen to yield a distal Bragg peak greater than or equal to the distal edge of the tumor. Finally the actual tumor area is defined by a collimator just ahead of the patient and a bolus shapes the field depth to account for the geometrical contour and inhomogeneities within the field volume. Scanning of the Bragg peak through the depth of the tumor, in order to yield a uniform dose to the tumor, will be achieved by varying the material ahead of the bolus during the exposure. This can be achieved by a range wheel, discrete range absorbers or an infinitely variable water absorber.

References

1. Tatsuaki Kanai et al., "Spot Scanning System for Proton Therapy" *Medical Physics* 7, 365 (1980).
2. E. V. Hungerford et al., "Proton Small Angle Multiple Scattering at 600 MeV," *Nuclear Physics* A197, 515 (1972).
3. V. L. Highland, "Some Practical Remarks on Multiple Scattering," *Nuc. Inst. and Methods* 129, 497 (1975).
4. S. L. Kramer, "Physics of Charged Particle Radiography" work in progress.
5. A. M. Koehler et al., "Flattening of Proton Dose Distributions for Large-Field Radiotherapy" *Medical Physics* 4, 297 (1977).

Table I. Parameters for Range-energy and Multiple Scattering of Protons

Material	K	n	Actual*	Calc.†	X_R	$\frac{dE}{dX} X_R$	$\frac{\Delta E}{\Delta E_{H_2O}}$
			$\left. \frac{dE}{dX} \right _{E=200MeV}$	$\left. \frac{dE}{dX} \right _{E=200MeV}$			
			MeV/gm/cm ²	MeV/gm/cm ²	gm/cm ²	MeV	
Water	32.2	0.564	4.56	4.43	36.1	164.9	1.0
Lucite	31.7	0.564	4.43	4.30	40.6	179.9	0.917
Al	27.1	0.570	3.54	3.42	24.01	84.9	1.94
Fe	25.0	0.575	3.19	3.09	13.84	44.2	3.73
Ag	22.05	0.584	2.74	2.68	8.9	24.4	6.76
Pb	18.7	0.596	2.27	2.23	6.4	14.5	11.4

*Energy loss for 200 MeV protons taken from W. H. Barkas and M. J. Berger in "Studies in Penetration of charged Particles in Matter," National Academy of Sciences, Nuclear Science Series Report # 39 (1964).

†Calculated energy loss from differentiating Eq. (4).

Table II. Parameters for Single Scatter Foil Proton Nozzle* (1 meter long)

Field Size	3 cm ϕ Field				8 cm ϕ Field				Units
	Lucite	Al	Fe	Pb	Lucite	Al	Fe	Pb	
$\langle \theta^2 \rangle^{1/2}$	65	65	65	65	174	174	174	174	mrad
X	23.9	22.6	16.9	9.7	26.2	33.2	36.0	38.5	gm/cm ²
L	199	83.6	21.4	8.5	222	123	45.8	33.9	mm
ΔE	144	95.0	58.7	22.5	199	192	172	106	MeV
ΔX_{H_2O}	22.7	17.0	11.7	4.9	25.4	25.4	24.7	18.9	cm
dE/dX Front	11.91	7.3	5.8	4.9	280	54.5	20.4	8.0	MeV/gm/cm ²

*Z1 = 1 meter, $E_0 = 200$ MeV, $dE/dX)_{E=200} = 4.43$ MeV/gm/cm²; efficiency = 5% \pm 2.5%
uniformity

X,L = thickness of scatter foil (in gm/cm², mm respectively)

ΔE = energy lost in foil

ΔX_{H_2O} = reduction of depth of penetration of beam from the initial 25.49 cm of H₂O

dE/dX = linear energy transfer at the entrance portal

Table III. Parameters for the High Efficiency-Large Field Proton Nozzle*

Field size	8 cm ϕ				20 cm ϕ				30 cm ϕ				45 cm ϕ				Units
	Lucite	Al	Fe	Pb	Lucite	Al	Fe	Pb	Lucite	Al	Fe	Pb	Lucite	Al	Fe	Pb	
θ_1 (mr)	9	9	9	9	23	23	23	23	35	35	35	35	53	53	53	53	mrad
θ_2 (mr)	6	6	6	6	14	14	14	14	21	21	21	21	31	31	31	31	
X1 gm/cm ²	1.39	0.83	0.48	0.23	7.43	4.83	2.91	1.39	13.6	9.8	6.18	3.06	20.7	17.7	12.2	6.59	gm/cm ²
L1 mm	11.7	3.1	0.6	0.2	63	17.9	3.7	1.2	115	36	7.8	2.7	175	65.7	15.6	5.8	mm
X2 gm/cm ²	0.46	0.28	0.17	0.08	1.99	1.48	0.94	0.47	2.67	2.59	1.86	1.00	2.08	3.39	3.11	2.05	gm/cm ²
L2 mm	3.9	1.0	0.2	0.1	16.9	5.5	1.2	0.4	22.6	9.6	2.4	0.9	17.6	122.7	4.0	1.8	mm
ΔE (MeV)	8.1	3.8	2.0	0.7	44.5	22.6	12.2	4.18	84.2	46.5	26.1	9.24	136	87.2	53.0	20.0	MeV
ΔX cm of H ₂ O	1.8	0.86	0.45	0.15	9.2	4.9	2.7	0.94	15.8	9.55	5.6	2.05	22.2	16.3	10.7	4.35	cmH ₂ O
dE/dX Front	4.57	4.49	4.46	4.44	5.37	4.85	4.65	4.50	6.75	5.43	4.93	4.59	10.7	6.89	5.61	4.80	MeV-cm ³ /gm
A ₁		27.5				68.9				103.4				155.2			mm
a ₁		5.5				13.8				20.7				31.0			mm
A ₀		11.6				29.0				43.4				65.2			mm
a ₀		2.3				5.8				8.7				13.0			mm
A ₂		110.0				275.6				413.6				620.8			mm
a ₂		22.0				55.2				82.8				124.0			mm

*Z₁ = 5 meters, Z₂ = 4 meters, Effic = 27% for $\pm 2.5\%$ dose uniformity

E_{Beam} = 200 MeV dE/dX)_{Beam} = 4.43 MeV/gm/cm² H₂O

Range (H₂O) = 25.49 cm

Table IV. Parameters for the High Efficiency - Small Field Proton Nozzle*

Field size	3 cm ϕ				8 cm ϕ				20 cm ϕ				Units
	Lucite	Al	Fe	Pb	Lucite	Al	Fe	Pb	Lucite	Al	Fe	Pb	
θ_1			9				23				59		mmrad
θ_2			8				22				55		mmrad
X_1	1.22	0.73	0.43	0.20	7.4	4.83	2.91	1.39	22.2	20.2	14.5	8.0	gm/cm ²
L_1	10.4	2.7	0.54	0.17	62.9	17.9	3.7	1.22	189	74.6	18.4	7.0	mm
X_2	1.03	0.63	0.37	0.17	4.6	3.6	2.36	1.19	2.96	6.84	7.62	5.91	gm/cm ²
L_2	8.7	2.3	0.50	0.20	39.3	13.4	3.0	1.0	25.1	25.3	9.7	5.2	mm
ΔE	9.9	4.7	2.48	0.83	58.8	30.7	16.8	5.82	122	122	80.8	32.9	MeV
ΔX_{H_2O}	2.2	1.06	0.56	0.2	11.7	6.53	3.67	1.30	24.5	20.7	15.3	6.9	cm H ₂ O
dE/dX	4.6	4.5	4.47	4.4	5.8	5.03	4.74	4.53	18.2	9.2	6.6	5.1	MeV-cm ³ /gm
A_0		0.43					1.15				2.90		cm
A_1		1.03					2.82				6.90		cm
A_2		4.14					11.03				27.6		cm
a_0		2.1					5.5				13.8		mm
a_1		5.2					13.8				34.5		mm
a_2		20.7					55.2				138		mm

* $Z_1 = 2m$, $Z_2 = 1 m$, Effic. = 27% for $\pm 2.5\%$ dose uniformity

$E_{Beam} = 200 \text{ MeV}$, $dE/dX = 4.43 \text{ MeV-cm}^2/\text{gm}$, Range (H₂O) = 25.49 cm

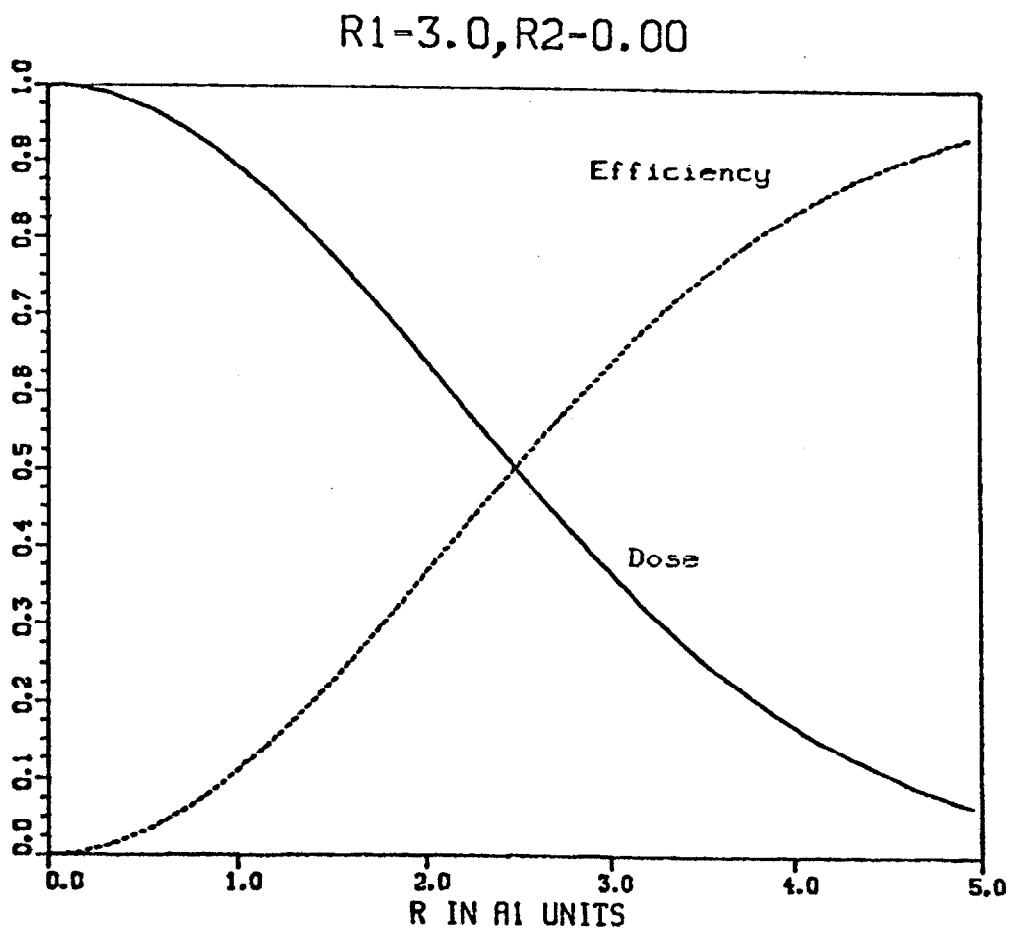


Fig. 1 Dose Distribution and Beam Efficiency for a single scatter foil proton nozzle (rms radius of the beam distribution = 3.0).

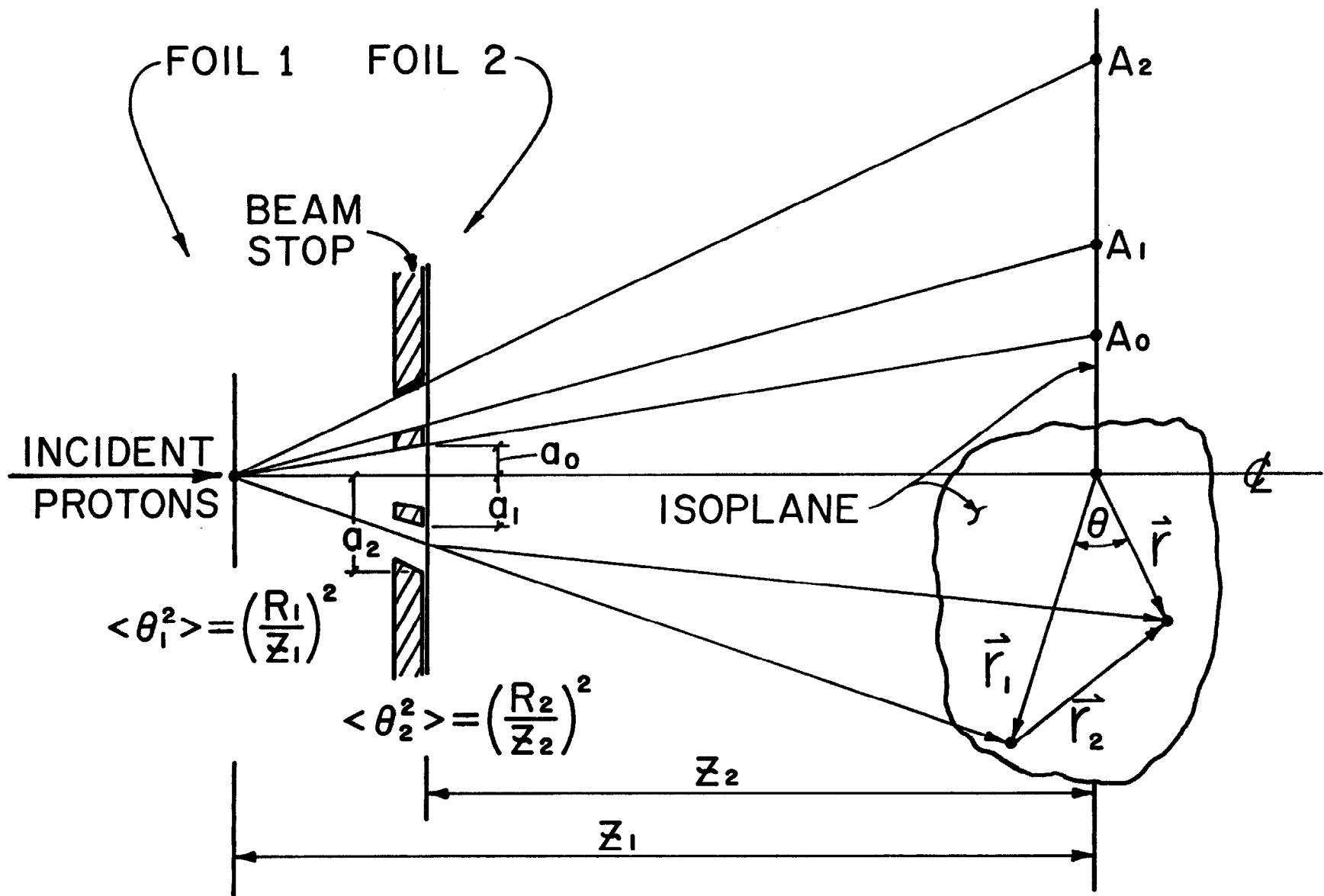


Fig. 2 Layout for a high efficiency nozzle.

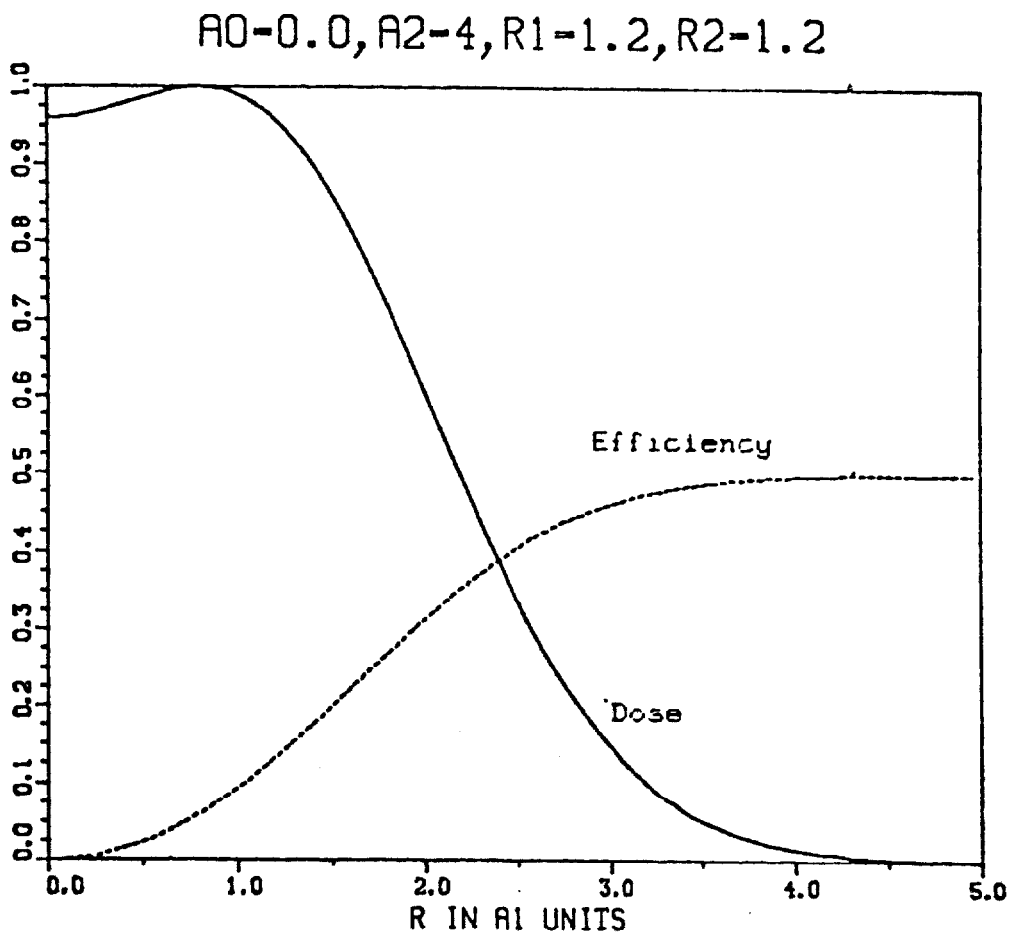


Fig. 3 Proton nozzle with two scattering foils and a solid inner beam stop.

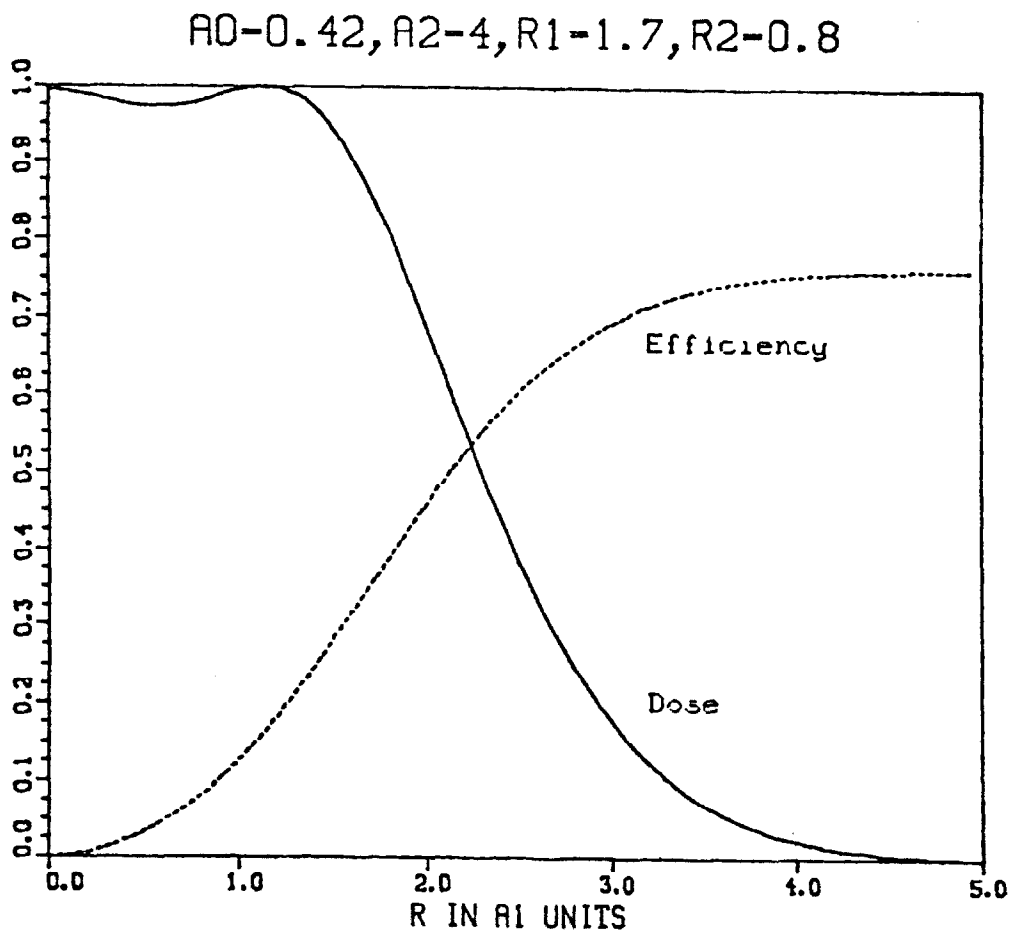


Fig. 4 High efficiency proton nozzle using two scattering foils.